Journal of Applied Mechanics and Technical Physics, Vol. 35, No. 1, 1994

CALCULATION OF THE VELOCITY PROFILE IN A NONLINEAR WAVE IN A FLUID LAYER FLOWING DOWN A VERTICAL WALL

P. I. Geshev and Kh. Kh. Murtazaev

UDC 532.62+532.594

A fluid flowing down a vertical surface due to gravity is an example of an active dissipative medium. The energy supply comes from the gravitational force while the dissipation comes from the viscous friction force. Studies of the linear stability of falling films of fluid [1, 2] have shown that smooth plane-parallel flow is unstable, no matter how small the Reynolds number. Usually motion in a film is considered laminar-wave flow up to Re $\cong$ 300-400 [3].

Almost all theoretical research has been done in the long-wavelength approximation, which corresponds to experimental data. It has been shown [4] that the long-wavelength approximation can be used up to Re $\cong$ 1000 for ordinary fluids. This approximation allows the complete system of the Navier–Stokes equations to be simplified to a boundary-layer system. An integral method [5] has been proposed which gives a semi-parabolic velocity profile. The assumption of self-similarity has been verified [6]. A system of two equations has been derived within the framework of the integral approach [7, 8]: one for the instantaneous thickness and one for the flow rate of the fluid for moderate Reynolds numbers. Stationary nonlinear running waves of the first kind, which are similar in form to sinusoidal waves, have been found from this approach [7, 8]. Highly nonlinear solutions of this system — which correspond to waves with a smoothly sloping tail, a steep front, and a capillary ripple ahead of the wave — can only be solved numerically [9, 10]. The development stages of both stimulated and naturally occurring waves, including two types of attractors, were examined [11] by extending an earlier theory [8, 12]. The theoretical results agreed quantitatively with experiment in the main part of the wave, but the capillary ripple, predicted by the integral approach, was much stronger and had a higher oscillation amplitude than in experiments.

Nonlinear theory has been examined and the velocity profile has been determined for waves of the first kind in the long-wavelength approximation for stationary running waves [13]. Stationary nonlinear solutions, based on boundary-layer equations and integral equations for describing film flow, give good agreement with experiment [14]; a detailed comparison is in progress. A transient solution of the Navier–Stokes equations has been done in the long-wavelength approximation for the initial stage of wave development, up to the occurrence of reverse flow in the thinnest part of the film [15].

Transient finite-element solutions for the complete system of Navier–Stokes equations have been found without any approximations [16]. A complete numerical solution using Galerkin's method has been presented for a stationary running wave in viscous fluid layers [17]. Calculations were done for various values of the dimensionless surface stress, including zero stress.

Here a new pseudospectral method is presented for calculating the transient development of a wave within the framework of the long-wavelength approximation. It can compute the complete development of the wave until it becomes stationary. This stationary wave is compared with the solution to the stationary equations. The solution is extended parametrically to large Reynolds numbers in order to determine the effect of Reynolds number on the wave characteristics. Solutions found for the long-wavelength approximation are compared with solutions [17] of the complete system of equations.

1. PROBLEM FORMULATION

A viscous incompressible fluid flows down a vertical plane by gravity. The flow is assumed to be two-dimensional and periodic with a wavelength λ. The x-axis is directed downward along the gravity-acceleration vector g; the y-axis is perpendicular to the surface. We will assume that the wavelength is much larger than the film thickness. As Nusselt showed, a falling fluid film always has a trivial stationary solution with a smooth plane-parallel free surface:

Novosibirsk. Translated from Prikladnaya Mekhanika i Tekhnicheskaya Fizika, No. 1, pp. 53-61, January-February, 1994. Original article submitted November 17, 1992; revision submitted February 16, 1993.

$$h(x) = \text{const},$$
$$u = (gh^2/2\nu)(2y/h - y^2/h^2) = u_0(2y/h - y^2/h^2),$$
$$q = gh^3/3\nu.$$

where h is the film thickness; u is the film velocity; $u_0 = gh^2/2\nu$ is the velocity on the film surface; q is the fluid flow rate; and ν is the kinematic viscosity.

In the long-wavelength approximation ($h/\lambda \ll 1$), a boundary-layer type system is obtained from the complete Navier–Stokes equations. We make it dimensionless by using $\langle h \rangle$ (the film thickness averaged over a wavelength), u_0 (the Nusselt velocity on the surface of an unperturbed film with thickness $\langle h \rangle$), and ρ (the fluid density). We map the motion onto the strip [0, 1] by transforming the transverse coordinate

$$\eta = 1 - y/h(x, t).$$

As a result, the transformed system of equations is written in the form

$$\frac{\partial u}{\partial t} + u\frac{\partial u}{\partial x} + \frac{1}{h}\frac{\partial u}{\partial \eta}\left((1-\eta)\frac{\partial h}{\partial t} + (1-\eta)u\frac{\partial h}{\partial x} - v\right) = \mathrm{We}\frac{\partial^3 h}{\partial x^3} + \frac{1}{\mathrm{Re}\,h^2}\frac{\partial^2 u}{\partial \eta^2} + \frac{2}{\mathrm{Re}},$$
$$\frac{\partial u}{\partial x} + \frac{(1-\eta)}{h}\frac{\partial h}{\partial x}\frac{\partial u}{\partial \eta} - \frac{1}{h}\frac{\partial u}{\partial \eta} = 0,$$

where u is the x-component of the velocity; v is the η-component of velocity; h is the instantaneous film thickness; $\mathrm{Re} = \frac{u_0\langle h \rangle}{\nu} = \frac{g\langle h \rangle^3}{2\nu^2}$ is the Reynolds number; $\mathrm{We} = \frac{\sigma}{\rho u_0^2\langle h \rangle} = \left(\frac{2}{\mathrm{Re}^5}\mathrm{Fi}\right)^{1/3}$ is the Weber number; $\mathrm{Fi} = \sigma^3/\rho^3 g\nu^4$ is the film number; and σ is the surface stress coefficient. The boundary conditions are as follows:

$$u = v = 0 \quad \text{for} \quad \eta = 1,$$
$$v = \frac{\partial h}{\partial t} + u\frac{\partial h}{\partial x} \quad \text{for} \quad \eta = 0,$$
$$\frac{\partial u}{\partial \eta} = 0 \quad \text{for} \quad \eta = 0.$$

The limits for integrating the continuity equation over η account for the no-slip condition for the transverse velocity:

$$v = (1-\eta)u\frac{\partial h}{\partial x} - \frac{\partial}{\partial x}\left(h\int_\eta^1 u\,d\eta\right).$$

From this equation and conservation of momentum, we obtain the equation for the film thickness

$$\frac{\partial h}{\partial t} + \frac{\partial}{\partial x}\left(h\int_0^1 u\,d\eta\right) = 0.$$

After several simple transformations, we eliminate the momentum boundary condition, and have the final system of two equations

$$\frac{\partial u}{\partial t} + u\frac{\partial u}{\partial x} + \frac{1}{h}\frac{\partial u}{\partial \eta}\left(\eta\frac{\partial}{\partial x}(h\int_0^1 u\,d\eta) - \frac{\partial}{\partial x}(h\int_0^\eta u\,d\eta)\right) = \mathrm{We}\frac{\partial^3 h}{\partial x^3} + \frac{1}{\mathrm{Re}\,h^2}\frac{\partial^2 u}{\partial \eta^2} + \frac{2}{\mathrm{Re}}; \tag{1.1}$$

$$\frac{\partial h}{\partial t} + \frac{\partial}{\partial x}\left(h \int_0^1 u \, d\eta\right) = 0. \tag{1.2}$$

The boundary conditions are as follows:

$$u = 0 \quad \text{for} \quad \eta = 1; \tag{1.3}$$

$$\frac{\partial u}{\partial \eta} = 0 \quad \text{for} \quad \eta = 0. \tag{1.4}$$

Complete formulation of the transient problem requires initial conditions for the functions u(x, η, t) and h(x, t):

$$u(x, \eta, 0) = f_0(x, \eta), \quad h(x, 0) = g_0(x).$$

These equations can only be solved numerically because of their high nonlinearity and complexity.

2. SOLUTION METHOD

Today there are no universal methods for solving nonlinear transient problems which describe the behavior of perturbations in active dissipative media. Here we decided to use relatively recent spectral and pseudospectral methods, which can be used for direct numerical modeling of turbulent flows [18]. In many cases, the effectiveness of the method depends on the proper choice of basis functions [19].

We seek solutions of the form

$$h(x, t) = \sum_{n=-N}^{N} h_n(t) \exp\{i\alpha n x\},$$

$$u(x, \eta, t) = \sum_{m=0}^{M} \sum_{n=-N}^{N} u_{mn}(t) \exp\{i\alpha n x\} T_m(\eta),$$

where the $T_m(\eta) = \cos(m \arccos \eta)$ are Chebyshev polynomials.

Chebyshev polynomials are used when the calculational points are concentrated near the wall, which is important in approximating steep velocity gradients. Their big advantage is that they are directly related to cosines and allow the use of rapid transform algorithms [20]. Chebyshev polynomials have been applied successfully for calculating stationary wave motion in films [17]. Here we used Galerkin's method to formulate a system of ordinary differential equations.

The system of Eqs. (1.1)-(1.4) is solved by a pseudospectral method, with a finite-difference approximation in time. The velocity is expanded only in even orders of Chebyshev polynomials, which satisfy the boundary condition (1.4) directly. It should be noted that using a spectral decomposition makes the system rigid, because of the discretization of the initial equations [21]; this requires using special finite-difference grids for integrating over time [22]. A characteristic of spectral methods is the occurrence of aliasing errors [23], which arise from cutting off the series in calculating nonlinear terms. This can lead to numerical instability due to error accumulation as the wave calculation proceeds. There are two methods to control this: increase the number of harmonics, which greatly increases computation time, or use filtering or smoothing [24]. Here we choose the second path. Filtering or smoothing was only used on the x-coordinate, which is directed along the flow. The following filter was used

$$f(k) = \begin{cases} 1, & k \leqslant k_0, \\ \exp(-a(k - k_0)^4), & k > k_0, \end{cases}$$

where k is the wave vector and a is a constant. The velocity and the thickness were filtered at each step. Only the stable modes, which should attenuate according to linear theory [1, 2], were suppressed. Smoothing was done with a five-point equation

$$f(x) = (-f(x-2\Delta x) + 4f(x-\Delta x) + 10f(x) + 4f(x+\Delta x) - f(x+2\Delta x))/16,$$

with which the filter, which corresponds to this operation, can be obtained via a Fourier transform. It was verified that the transform also suppressed the stable modes. The number of time steps between smoothing was chosen by experiment. If it was done on every step, the smoothing would not bring out the high-frequency part of the spectrum; therefore, the wave profile would differ only weakly from a sine wave.

Most of the solutions here were smoothed in this way. Filtered and smoothed solutions agree satisfactorily over most of the wave. Actually, smoothing or filtering introduces additional dissipation, which can suppress the numerical instabilities which arise from the inaccuracies in calculating nonlinear terms and spatial variables. The stationary problem was solved in order to test the solution to the transient problem.

Let the solution to the initial system (1.1)-(1.4) be a stationary running wave

$$h(x, t) = h(x - ct), \quad u(x, \eta, t) = u(x - ct, \eta).$$

Then the equations can be represented in the form

$$(-c + u)\frac{\partial u}{\partial x} + \frac{1}{h}\frac{\partial u}{\partial \eta}\left(\eta \frac{\partial}{\partial x}\left(h\int_0^1 u\, d\eta\right) - \frac{\partial}{\partial x}\left(h\int_0^\eta u\, d\eta\right)\right) - \mathrm{We}\frac{\partial^3 h}{\partial x^3} - $$
$$- \frac{1}{\mathrm{Re}\, h^2}\frac{\partial^2 u}{\partial \eta^2} - \frac{2}{\mathrm{Re}} = 0; \tag{2.1}$$

$$h\left(-c + \int_0^1 u\, d\eta\right) - A = 0, \text{ where } A = \text{const}; \tag{2.2}$$

$$u = 0 \quad \text{for} \quad \eta = 1. \tag{2.3}$$

As noted previously, using only even-order Chebyshev polynomials satisfies the boundary condition (1.4). The boundary condition (2.3) will be fulfilled by the τ-method [23]: in essence the coefficient for the last harmonic is determined directly from the boundary condition (2:3). Because $T_m(1) = 1$, then

$$\sum_{m=0}^{M} u_{mn} = 0.$$

from which the last mode can be expressed as

$$u_{Mn} = \sum_{m=0}^{M-2} u_{mn}, \quad |n| \leq N.$$

Let $\xi = x - ct$, then

$$h(\xi) = \sum_{n=-N}^{N} h_n \exp\{i\alpha n\xi\},$$
$$u(\xi, \eta) = \sum_{m=0}^{M}\sum_{n=-N}^{N} u_{mn} \exp\{i\alpha n\xi\}\, T_m(\eta).$$

Application of the spectral method leads to a system of nonlinear equations for the decomposition coefficients h_n and u_{mn}. We obtain a system of equations of the type

$$F_i(h_{-N}, \ldots, h_n, \ldots, h_N, \ldots, u_{mn}, \ldots, u_{MN}, c, A) = 0. \tag{2.4}$$

In formulating the problem, the average film thickness was fixed; therefore h_0 is known. We also specify $\mathrm{Im}(h_1)$ equal to the value from the steady-state solution to the transient problem (this is not fundamental, but is convenient for further comparison). From this we obtain the missing equations in A and c.

We write Eqs. (2.4) in the form

$$F_i(x_1, x_2, \dots, x_k) = 0.$$

This system is solved by Newton's method

$$\left.\frac{\partial F_i}{\partial x_j}\right|_{x=x^0} \Delta x_j = -F_i(x_j^0)$$

where x_j^0 is the initial approximation. If x_j^0 is in the attractor region of the solution, then the process converges. The Jacobian matrix is calculated by a finite-difference method:

$$\left.\frac{\partial F_i}{\partial x_j}\right|_{x=x^0} = \frac{F_i(x_1^0, \dots, x_j^0 + \Delta x_j^0, \dots, x_k^0) - F_i(x_1^0, \dots, x_k^0)}{\Delta x_j^0},$$

and the function F_i itself is calculated by the pseudospectral method.

The initial approximation is taken to be the stationary solution obtained by solving the transient problem — Eqs. (2.1)-(2.3). The solution is extended parametrically to large Reynolds numbers; i.e., the increments in the Reynolds numbers are chosen so small that Newton's iteration converges. The initial solution for the new Reynolds number is the solution for the previous Reynolds number.

3. RESULTS OF THE CALCULATIONS

Two fluids were used in the calculations: water and a water–glycerine mixture. For water, $\nu = 1.03 \cdot 10^{-6}$ m^2/sec and $\sigma/\rho = 72.9 \cdot 10^{-6}$ m^3/sec^2; for the water–glycerin mixture, $\nu = 4.9 \cdot 10^{-6}$ m^2/sec and $\sigma/\rho = 59 \cdot 10^{-6}$ m^3/sec^2. The same parameters were used as in [17], so the results from [17] could be compared.

In solving the transient problem, the initial condition was chosen to be a sinusoidal perturbation of the film surface with a wavelength λ and an amplitude of 0.3-0.5. The initial velocity profile was specified to be semi-parabolic. The amplitude decreased during the initial wave development. After the wave formed a sharp enough front, the amplitude started to increase. A capillary ripple started when the steepness of the front reached its maximum. After this the wave became stationary. During the calculations we computed the flow Reynolds number Re_q, which is used by most authors:

$$\mathrm{Re}_q = Q/\nu$$

where $Q = \frac{1}{\lambda}\int_0^\lambda dx \int_0^h u\, dy$ is the average flow rate. As can be seen, Re_q is not specified initially, but is established as the transient develops. Therefore it is not easy to compare the calculated stationary solution with the stationary running waves obtained by other investigators within the framework of an integral model, where Re_q is usually specified.

Depending on the initial perturbation wavelength, two types of waves develop. For small wavelengths, the resultant wave is close to the sinusoid in Fig. 1 (Re = 8.75, We = 11.23, and λ = 30). At larger wavelengths the wave has a gently sloping tail and a steep front, with a capillary ripple ahead of the front (Fig. 2: Re = 15.5, We = 42.82, λ = 98, Re_q = 10.96, and c = 2.08). In Fig. 2 the dashed curve shows the solution of the stationary Eqs. (2.1)-(2.3) (for Re_q = 10.97 and c = 2.10), where the initial approximation was the result of the transient development. The agreement is very good. In these calculations 64 harmonics were taken along the Ox axis, while the solution along the Oy axis was approximated by an eighth-order polynomial. Actually, the last two coefficients in the polynomial went to zero. Other cases of transient development to a stationary wave are shown in Fig. 3 (Re = 8.75, We = 11.23, λ = 98, Re_q = 6.10, and c = 2.11) and Fig. 4 (Re = 30,

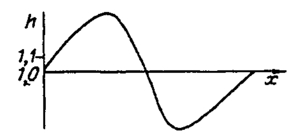

Fig. 1

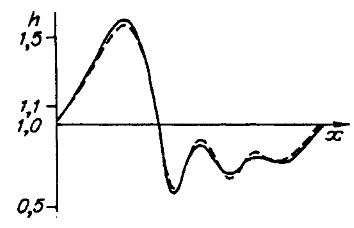

Fig. 2

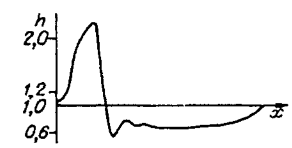

Fig. 3

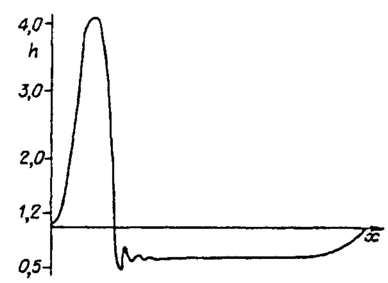

Fig. 4

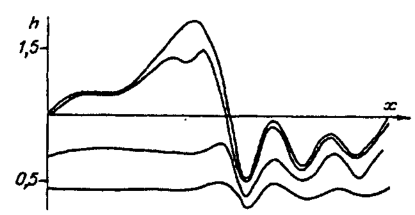

Fig. 5

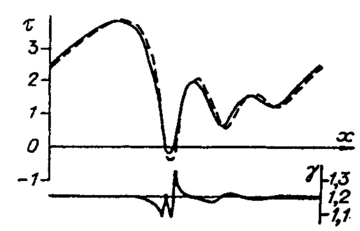

Fig. 6

We = 1.44, λ = 98, Re_q = 15.56, and c = 1.98). Figure 4 shows the case of large Reynolds numbers. As can be seen, the wave amplitude $\cong$ 5. These large amplitudes are not found in the linear theory. It should be noted that when this solution is used as an initial approximation, the Newton iteration method for solving the stationary equations did not converge. Evidently there are no stationary solutions at such large Reynolds numbers, but a quasi-stationary form of the type shown in Fig. 4 appears; or else the wave cannot attain such a form and decays into three-dimensional waves. In this case velocity profile is nowhere near semi-parabolic, and strong vortex flows arise near the peak of the wave.

New stationary solutions were sought by parametric extrapolation from a stationary solution like the one in Fig. 2. Figure 5 (Re = 22, We = 23.89, λ = 98, Re_q = 17.95, and c = 2.01) shows such a solution, and also the flow lines. A "drop" which hardly moves (in the coordinate system that moves with the phase velocity of the wave) can be seen at the peak of the wave; such a drop is found experimentally. Figures 2 and 5 show a large precursor peak ahead of the wave front as Re increases, which is not predicted by the integral theory. As Re increases, the difference from the semi-parabolic velocity profile constantly increases, and becomes larger as the wave becomes steeper.

The solid curves in Figs. 6 and 7 show the dimensionless quasistatic friction $\tau_q = 3\langle u\rangle/h$ for the stationary solutions in Figs. 2 and 5; τ_q is used in the approximate calculations of film flow [7, 8]. The dashed curves show the actual friction $\tau = (\partial u/\partial\eta)|_{\eta=1}$. The lower curves on the same figures show the integral form factor $\gamma(x) = \langle u^2\rangle/\langle u\rangle^2$. In the main part of the wave γ is close to 1.2, but γ initially decreases where the film thickness changes rapidly, indicating a more rapidly changing velocity profile than parabolic, and then increases, as for linear profiles. The pulsations in the minimum-thickness region can be explained by the fact that the velocity is small and negative in this region. A zone of negative velocities also appeared in other calculations [15]. In our calculations for highly nonlinear waves with a developed capillary ripple, the velocity was always negative over

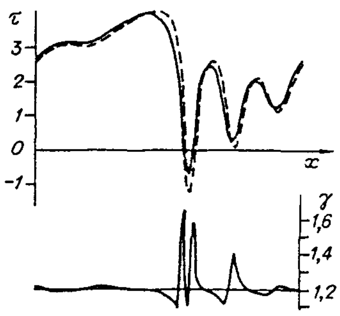

Fig. 7

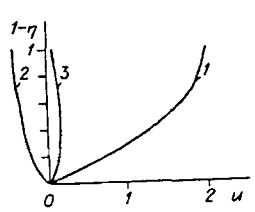

Fig. 8

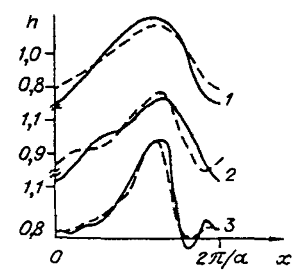

Fig. 9

the whole cross section in the region of minimum film thickness. This phenomenon is unexpected and evidently is caused by surface-tension forces. This zone has been discussed in detail [14]. The same curves show that the deviation from a semi-parabolic velocity profile also increases as Re increases. Figure 8 shows the velocity profile for the case in Fig. 5 (curve 1 corresponds to the velocity profile in the section with maximum film thickness, curve 2 is for minimum film thickness, and curve 3 is where the film thickness drops rapidly near the minimum). Curve 3 shows the inflection in the velocity profile which appears if the Reynolds numbers are large enough.

The stationary solution obtained by the schlieren method in the long-wavelength approximation has been compared directly with solutions from integral theory and with experiment [14]. Therefore it is interesting to compare our solution of the system of boundary-layer equations with solutions of the complete system of Navier–Stokes equations. In a previous investigation [17], most of the Navier–Stokes solutions were for small values of the dimensionless surface tension, where the transverse velocity component is large and the boundary-layer approximation is in doubt. Figure 9 compares the stationary solutions for Re = 3.27 and $Fi^{1/3} = 50$. Curves 1-3 correspond to waves for $\alpha = 0.864$, 0.643, and 0.437 (α is the ratio of the wave number to the neutral wave number from linear stability theory); the solid curves are solutions in the long-wavelength approximation, and the dashed curves are for the complete solution [17]. Stationary solutions of the system (1.1)-(1.4) were obtained as the transient developed. Then they were refined with the solution of the stationary Eqs. (2.1)-(2.3) by using the solution from the transient solution as the initial approximation in Newton's method. The curves show that the solutions are close to each other, but still differ rather substantially for these parameter values.

In conclusion, a numerical method was developed which calculates the transient development of initially smooth perturbations in the long-wavelength approximation until they become stationary. The main stage of the wave development corresponds qualitatively to that computed [11] by the integral model [7, 8]. It can be confirmed that the resultant stationary running waves are stable, because they are established during the development of the transient.

Stationary running-wave solutions were obtained by using the solution of the transient problem as the initial approximation in Newton's method. They were numerically extrapolated to larger Reynolds numbers. A new family of solutions was found with a large peak ahead of the tail of the wave.

We confirmed the existence of a narrow region of negative velocities, which also appears in linear theory, but still has not been observed experimentally.

Comparison of the resultant solutions with solutions to the complete system of equations shows that the long-wavelength approximation can change the shape of the solution substantially when the dimensionless surface stresses are small.

When Re $\leq$ 20, the semiparabolic approximation is valid. The basic difference appears where the steepness of the wave is at a maximum and increases with increasing Re.

REFERENCES

1. G. W. Benjamin, "Wave formation in laminar flow down an inclined plane," J. Fluid Mech., **2**, 554-574 (1957).
2. Ch.-S. Yin, "Stability of liquid flow down an inclined plane," Phys. Fluids, **6**, No. 3 (1963).
3. P. L. Kapitsa and S. P. Kapitsa, "Wave flow of thin layers of a viscous fluid. 3. Experimental study of the wave regime," Zh. Éksp. Teor. Fiz., **19**, No. 2 (1949).
4. V. S. Krylov, V. P. Vorotilin, and V. G. Levich, "Theory of wave motion of thin fluid films," Teor. Osn. Khim. Tekhnol., **3**, No. 47 (1969).
5. P. L. Kapitsa, "Wave flow of thin layers of a viscous fluid," Zh. Éksp. Teor. Fiz., **18**, No. 1 (1948).
6. C. D. Berbente and E. Ruckenstein, "Hydrodynamics of wave flow," AIChE J., **14**, No. 5 (1968).
7. V. Ya. Shkadov, "Wave flow of a thin layer of a viscous fluid by gravity," Izv. Akad. Nauk Mekh. Zhidk. Gaza, No. 1 (1967).
8. V. Ya. Shkadov, "Theory of wave flows of a thin layer of a viscous fluid," Izv. Akad. Nauk Mekh. Zhidk. Gaza, No. 2 (1968).
9. A. V. Bunov, E. A. Demekhin, and V. Ya. Shkadov, "The nonuniqueness of nonlinear wave solutions in a viscous layer," Prikl. Mat. Mekh., **48**, No. 4 (1984).
10. Yu. Ya. Trifonov and O. Yu. Tsvelodub, "Wave regimes in falling fluid films," in: Hydrodynamics and Heat and Mass Transfer of Flows of a Fluid with a Free Surface: Collection of Scientific Works [in Russian], Novosibirsk (1985).
11. E. A. Demekhin, G. Yu. Tokarev, and V. Ya. Shkadov, "Two-dimensional transient waves in a vertical fluid film," Teor. Osn. Khim. Tekh., **21**, No. 2 (1987).
12. E. A. Demekhin and V. Ya. Shkadov, "Transient waves in a layer of viscous fluid," Izv. Akad. Nauk Mekh. Zhidk. Gaza, No. 3 (1981).
13. V. Ya. Shkadov, L. P. Kholpanov, V. A. Malyusov, and N. M. Zhavoronkov, "Nonlinear theory of wave flows of a fluid film," Teor. Osn. Khim. Tekh., **4**, No. 6 (1970).
14. E. A. Demekhin, M. A. Kaplan, and V. Ya. Shkadov, "Mathematical models of the theory of thin films of a viscous fluid," Izv. Akad. Nauk Mekh. Zhidk. Gaza, No. 6 (1987).
15. P. I. Geshev and B. S. Ezdin, "Calculation of the velocity profile and wave shape in a falling fluid film," in: Hydrodynamics and Heat and Mass Transfer of Flows of a Fluid with a Free Surface: Collection of Scientific Works [in Russian], Novosibirsk (1985).
16. P. Bach and J. Villadsen, "Simulation of the vertical flow of a thin, wavy film using a finite-element method," Int. J. Heat Mass Transfer, **27**, No. 6 (1984).
17. E. A. Demekhin and M. A. Kaplan, "Construction of accurate numerical solutions for stationary running waves in thin layers of a viscous fluid," Izv. Akad. Nauk Mekh. Zhidk. Gaza, No. 3 (1990).
18. S. A. Orszag and G. S. Patterson, "Numerical simulation of three-dimensional homogeneous isotropic turbulence," Phys. Rev. Lett., **28**, No. 1 (1972).
19. S. A. Orszag and M. Israeli, "Numerical simulation of viscous incompressible flows," Annual Review of Fluid Mech., Palo Alto, CA (1974), Vol. 6, p. 281.
20. V. A. Gaponov, "Fast Fourier transform package with application to modeling random processes," Preprint No. 14-76 [in Russian], Academy of Sciences, Siberian Division, Institute of Thermal Physics, Novosibirsk (1976).
21. D. Gottlieb and L. Lustman, "The Dufort–Frankel Chebyshev method for parabolic initial-boundary problems," Computers and Fluids, **11**, No. 2 (1983).
22. C. W. Gear, Numerical Initial Value Problems in Ordinary Differential Equations, Prentice Hall, Englewood Cliffs, NY (1971).
23. U. Shuman, G. Gretzbach, and L. Clauser, Direct Methods of Numerical Modeling of Turbulent Flows [Russian translation], Mir, Moscow (1984).
24. R. Perrey and T. D. Taylor, Numerical Methods in Problems of Fluid Mechanics [Russian translation], Gidrometeioizdat, Leningrad (1986).